Fermi National Accelerator Laboratory

FERMILAB-Conf-94/158-E

CDF

Electroweak Boson Pair Production at CDF

S. Errede et. al
The CDF Collaboration

Fermi National Accelerator Laboratory
P.O. Box 500, Batavia, Illinois 60510

June 1994

Submitted to the *27th International Conference on High Energy Physics*, Glasgow, Scotland, July 20-27, 1994

Operated by Universities Research Association Inc. under Contract No. DE-AC02-76CHO3000 with the United States Department of Energy

Disclaimer

This report was prepared as an account of work sponsored by an agency of the United States Government. Neither the United States Government nor any agency thereof, nor any of their employees, makes any warranty, express or implied, or assumes any legal liability or responsibility for the accuracy, completeness, or usefulness of any information, apparatus, product, or process disclosed, or represents that its use would not infringe privately owned rights. Reference herein to any specific commercial product, process, or service by trade name, trademark, manufacturer, or otherwise, does not necessarily constitute or imply its endorsement, recommendation, or favoring by the United States Government or any agency thereof. The views and opinions of authors expressed herein do not necessarily state or reflect those of the United States Government or any agency thereof.

CDF/PUB/ELECTROWEAK/PUBLIC/2637
FERMILAB-CONF-94/158-E

ICHEP-94
gls0375
contributed for sessions pa-01, pl-02

Electroweak Boson Pair Production at CDF

The CDF Collaboration*

Abstract

Preliminary results from CDF on $W+\gamma$, $Z+\gamma$ and W^+W^-, WZ, ZZ boson pair production in $\sqrt{s}=1.8$ TeV $\bar{p}$-p collisions from the 1992-93 collider run are presented. Measurements of the production cross section $\times$ decay branching ratios $\sigma * B(W+\gamma)$ and $\sigma * B(Z+\gamma)$ have been obtained. The cross section ratios $\mathcal{R}(W\gamma/W)$, $\mathcal{R}(Z\gamma/Z)$, $\mathcal{R}(W\gamma/Z\gamma)$ and $\mathcal{R}(W/Z)$ are discussed. We extract direct limits on $\mathcal{CP}$-conserving and $\mathcal{CP}$-violating $WW\gamma$, WWZ, $ZZ\gamma$ and $Z\gamma\gamma$ anomalous couplings. In the static limit, the direct experimental limits on $WW\gamma$ and $ZZ\gamma$ anomalous couplings are related to bounds on the higher-order static (transition) EM moments of the W (Z) bosons. Expectations from the on-going and future Tevatron collider runs are discussed.

Contributed paper to the 27th International Conference on High Energy Physics
Glasgow, Scotland July 20-27, 1994

*Contact person: Steven Errede, SERREDE@fnald.fnal.gov

During the 1992 Tevatron collider run, the Collider Detector at Fermilab (CDF) accumulated ~ 20 pb^{-1} of integrated luminosity. The statistics of the inclusive W and Z data samples obtained during this run ($\sim 20K$ W and $\sim 2K$ Z events) are sufficiently large that studies of rare and/or semi-rare exclusive processes such as $W+\gamma$, $Z+\gamma$, WW, WZ and ZZ-pair production are now becoming feasible.

The observation and detailed study of these processes provides important new tests of the Standard Model (SM) of electroweak interactions through the investigation and study of tri-linear gauge boson couplings of the W, Z and γ. Strong gauge cancellations are predicted to occur in the $W+\gamma$, WW and WZ processes, while no such cancellations are expected for the $Z+\gamma$ or ZZ processes. The tri-linear gauge boson couplings associated with the $WW\gamma$ and WWZ vertices (s-channel Feynman diagrams) are a consequence of the non-Abelian $SU_L(2) \times U_Y(1)$ symmetry of the electroweak theory [1]. They are the *only* tri-vector boson vertices allowed in the SM. The corresponding u and t-channel di-boson processes depend only on the coupling between quarks and electroweak bosons. However, the fermion-gauge boson couplings are now well-tested in the production and decay of single bosons, and are considered to be known. Therefore, we may regard di-boson production as primarily a test of the strength and nature of the tri-linear gauge boson couplings. The cancellation between the s, t and u-channel amplitudes in the $W+\gamma$ process results in the prediction of a radiation amplitude zero [2] in the $W^{\pm}\gamma$ center of mass angular distribution at $\cos\theta^* = \mp 1/3$. This can also be observed as a dip in the photon$-$lepton pseudorapidity difference distribution $\Delta\eta_{\gamma-\ell^{\pm}} \simeq \mp 0.3$ in $\sqrt{s} = 1.8$ TeV $\bar{\text{p}}$-p collisions [3]. A similar amplitude zero is predicted in $W^{\pm}Z$ production [4].

In various non-standard models of the electroweak interactions, the W, Z and γ are viewed as composite, rather than fundamental particles [5]. In such scenarios, non-standard $WW\gamma$, WWZ, $ZZ\gamma$, $Z\gamma\gamma$ and ZZZ anomalous couplings may exist. New physics must be introduced at large $\sqrt{\hat{s}}$ [6] in order to avoid violation of (tree-level) S-matrix unitarity [7]. The anomalous couplings are modified via the introduction of a (generalized dipole) form factor which forces the anomalous boson couplings to approach their SM values at large $\sqrt{\hat{s}}$. The form factor scale Λ_{FF} is presumed to be larger than the typical $\sqrt{\hat{s}}$ values seen at the Tevatron. A signature of the existence of non-zero anomalous boson couplings is an excess rate of production of di-boson pairs, particularly at high transverse energies. The absence of an excess of such events can therefore be used to obtain *direct* experimental limits on such anomalous couplings for each di-boson process.

The CDF detector is described in detail elsewhere [8]. The detector components most relevant to this analysis are the vertex time projection chamber (VTX) for measuring the position of the primary vertex, the central tracking chamber (CTC) immersed in a 1.4 T solenoidal magnetic field for charged particle momentum measurement, the central EM and hadron calorimeters (CEM and CHA) for energy measurement, the central muon system (CMU) and central muon upgrade (CMUP) for muon identification, and the plug and forward EM and hadron calorimeters (PEM and PHA, FEM and FHA) for energy measurement. The calorimeters are arranged in projective towers and cover the pseudorapidity range $|\eta| < 1.1$ in the central region, $1.1 < |\eta| < 2.4$ in the plug region, and $2.4 < |\eta| < 4.2$ in the forward region. In the central EM calorimeter, highly-segmented strip chambers located at shower maximum (~ 6 r.l.) are used for measurement of transverse shower profiles associated with electrons and photons. The central muon chambers cover the pseudorapidity range $|\eta| < 0.6$.

The inclusive electron W and Z data samples were collected using a $E_T > 16$ GeV electron trigger. The inclusive muon W and Z data samples were collected using a $P_T > 9$ GeV/c muon trigger. Offline, the inclusive electron W data sample was obtained by requiring events with an isolated electron in a good fiducial region of the central calorimeter, with transverse energy $E_T > 20$ GeV, good 3-D track matching with the CES shower centroid, low longitudinal shower leakage into the hadron calorimeter, and missing transverse energy $\not\!\!E_T > 20$ GeV [9]. A total of 13920 events passed the electron W requirements. The inclusive muon W data sample was obtained by requiring events with an isolated track with $P_T > 20$ GeV/c matched to a track stub in a good fiducial region of the CMU and CMUP chambers and a minimum ionizing signature in the calorimeter [10]. A total of 6105 events passed the muon W requirements. The inclusive electron and muon Z data samples were obtained using the same lepton identification requirements as above, and less restrictive criteria for the second lepton. The inclusive electron Z data sample required a second electron with $E_T > 20$, 15 or 10 GeV if in the CEM, PEM or FEM regions of the CDF calorimeters, respectively, and a di-electron pair mass of $70 < M_{e^+e^-} < 110$ GeV/c^2. In the central region, where tracking information is available, the second electron must also have $0.5 < E/P < 2.0$ and opposite charge to the first lepton. A total of 1237 events passed the electron Z requirements. The inclusive muon Z data sample required a second muon with $P_T > 20$ GeV/c, of opposite charge to the first, and a di-muon pair mass of $65 < M_{\mu^+\mu^-} < 115$ GeV/c^2. A total of 507 events passed the muon Z requirements.

$W + \gamma$ and $Z + \gamma$ Boson Pair Production at CDF

$W + \gamma$ and $Z + \gamma$ boson pair candidates were obtained from the inclusive W and Z data samples by requiring an isolated central photon within the fiducial region of the CDF calorimeters and with $E_T^\gamma \geq 7$ GeV. An angular separation between the charged lepton and the photon of $\Delta R_{\ell\gamma} > 0.7$ was required to suppress contributions from final-state bremsstrahlung. To reduce QCD background from W/Z+jets, the excess transverse energy in a cone of $\Delta R = 0.4$ around the EM cluster was required to be less than 15% of the EM cluster E_T, and the sum of the P_T of all charged tracks within this cone was required to be less than 2.0 GeV/c. Events with a track pointing directly at the EM cluster were rejected. To reduce the background from neutral hadrons, the ratio of hadronic to electromagnetic energy in the EM cluster was required to be less than $0.055 + 0.00045 * E$, where E was the total energy of the EM cluster in GeV. To suppress π^0 and multi-photon backgrounds, the lateral shower shape of the cluster was required to be consistent with that of a single particle. Events having more than one CES cluster with energy > 1.0 GeV associated with the EM calorimeter cluster were rejected. Using these selection criteria 18 (7) $W + \gamma$ candidates and 4 (4) $Z + \gamma$ candidates were found in the inclusive electron (muon) W/Z data samples, respectively.

The level of background in each of the four data samples due to QCD jet production in association with a W or Z boson was determined by use of a non-signal control sample of jet data. The QCD jet fragmentation probability distribution $\mathcal{P}(J \to \gamma)$ as a function of E_T was determined from this data sample. A correction for the (statistical) removal of prompt, isolated photons in this control sample of jets was made using a shower shape analysis. The probability was found to be $\mathcal{P}(J \to \gamma) \sim 8 \times 10^{-4}$ at $E_T = 9$ GeV, decreasing exponentially to $\sim 10^{-4}$ at $E_T = 25$ GeV. The QCD jet fragmentation probability distribution was then convoluted with the central jet E_T spectrum in each of the four inclusive W/Z data samples to obtain an estimate of the QCD background of 4.6 ± 1.8 $(stat + syst)$ $(1.9 \pm 0.6$ $(stat + syst))$ events in the electron (muon) $W + \gamma$ data

samples, respectively, and 0.4 ± 0.2 ($stat + syst$) (0.10 ± 0.05 ($stat + syst$)) events in the electron (muon) $Z + \gamma$ data samples, respectively. These results are in good agreement with those obtained from VECBOS [11] $W/Z + n$ Jets Monte Carlo simulations. In the $W + \gamma$ data samples, the contribution from the $Z + \gamma$ process where one of the leptons from Z decay is not detected is also significant. This background was suppressed by using a "no-2^{nd} track" cut, removing events with isolated tracks of opposite charge to that of the W decay lepton and with $P_T > 10$ GeV/c. A total of 0.43 ± 0.02 ($stat + syst$) (1.14 ± 0.06 ($stat + syst$)) $Z + \gamma$ background events are expected in the electron (muon) $W + \gamma$ data samples, respectively, using the Baur $Z + \gamma$ Monte Carlo event generator [12] and a detailed CDF detector simulation. In addition, we used the Baur $W + \gamma$ Monte Carlo [13] for estimating the $W + \gamma$ "background" from $W \rightarrow \tau \rightarrow \ell\nu\bar{\nu}$ ($\ell = e,\ \mu$) decays passing our event selection criteria. In the electron (muon) $W + \gamma$ data samples, 0.29 ± 0.02 ($stat + syst$) (1.14 ± 0.06 ($stat + syst$)) events are expected, respectively from τ decay channel in $W + \gamma$ production. In the electron/muon $Z + \gamma$ data samples, the contribution from the $Z \rightarrow \tau^+\tau^-$ decay channel is negligibly small.

The Baur $W + \gamma$ and $Z + \gamma$ Monte Carlo event generator programs [13, 12], coupled with a detailed MC simulation program of the CDF detector were used to obtain the SM predictions for the $W + \gamma$ and $Z + \gamma$ data samples for $E_T^\gamma > 7$ GeV and $\Delta R_{\ell\gamma} > 0.7$. The MRSD-' [14] structure functions were used for event generation as they best match the most recent W decay lepton charge asymmetry measurements from CDF [15]. The observed event yield and the SM prediction for the individual and combined $e + \mu$ $W + \gamma$ and $Z + \gamma$ results are summarized in Table 1. The experimental results are in good agreement with SM expectations.

Channel	$\mathcal{N}_{obs}$	$\Sigma\mathcal{N}_{bkgnd}$	$\mathcal{N}_{signal}$	$\mathcal{N}_{SM}$
e $W\gamma$	18	5.3 ± 1.8	12.7 ± 4.6	15.4 ± 0.7
μ $W\gamma$	7	3.2 ± 0.6	3.8 ± 2.7	7.9 ± 0.4
$e + \mu$ $W\gamma$	25	8.5 ± 1.9	16.5 ± 5.4	23.3 ± 1.1
e $Z\gamma$	4	0.4 ± 0.2	3.6 ± 2.0	4.3 ± 0.2
μ $Z\gamma$	4	0.1 ± 0.1	3.9 ± 2.0	2.8 ± 0.1
$e + \mu$ $Z\gamma$	8	0.5 ± 0.2	7.5 ± 2.8	7.1 ± 0.3

Table 1: Summary of $W + \gamma$ and $Z + \gamma$ results. The observed number of events $\mathcal{N}_{obs}$, predicted number of total background events $\Sigma\mathcal{N}_{bkgnd}$, number of signal events $\mathcal{N}_{signal} = \mathcal{N}_{obs} - \Sigma\mathcal{N}_{bkgnd}$ and predicted number of SM signal events, $\mathcal{N}_{SM}$ for each channel are given. The statistical and systematic uncertainties associated with $\Sigma\mathcal{N}_{bkgnd}$, $\mathcal{N}_{signal}$ and $\mathcal{N}_{SM}$ are given for each channel.

The SM predictions for $W + \gamma$ and $Z + \gamma$ production cross section $\times$ branching ratios are summarized in Table 2. The experimental results are in good agreement with SM expectations. The systematic uncertainties in the SM predictions and the experimental measurements include contributions from structure function choice, Q^2-scale uncertainties, uncertainties associated with the $W/Z + \gamma$ P_T-distribution [16] and higher-order QCD corrections [17]. The experimental results also include the luminosity uncertainty, lepton/photon identification efficiency uncertainties, and

kinematic and geometrical acceptance uncertainties. A small correction to the e/μ $Z+\gamma$ result has been applied to remove the Drell-Yan contribution.

Channel	$\sigma \cdot B(V_\ell+\gamma)_{expt}$ (pb)	$\sigma \cdot B(V_\ell+\gamma)_{SM}$ (pb)
e $W\gamma$	15.3 ± 5.7	
μ $W\gamma$	9.0 ± 6.4	18.6 ± 2.8
$e+\mu$ $W\gamma$	13.2 ± 4.4	
e $Z\gamma$	4.0 ± 2.3	
μ $Z\gamma$	6.6 ± 3.4	5.2 ± 0.6
$e+\mu$ $Z\gamma$	5.1 ± 1.9	

Table 2: Summary of $\sigma \cdot B(V_\ell+\gamma)$ results ($V = W$ or Z). The statistical and systematic uncertainties for $\sigma \cdot B(V_\ell+\gamma)_{expt}$ and $\sigma \cdot B(V_\ell+\gamma)_{SM}$ are given.

Figures 1-3 compare kinematic distributions for the combined $e+\mu$ $W+\gamma$ data with Standard Model predictions and background. The falling spectrum of the $\Delta R_{\ell\gamma}$ distribution in Fig. 2 indicates that the largest contribution to our signal is from radiative W decays. The cluster transverse mass distribution (also known as the minimum invariant mass) [18] is shown in Fig. 3. It contains 6 $e+\mu$ $W+\gamma$ candidate events with $M_{CT}^{W} > 90$ GeV/c^2, which are produced primarily by the direct W-photon coupling. The observed rate is consistent with the Standard Model expectation of 8.5 events.

Figures 4-6 compare kinematic distributions for the combined $e+\mu$ $Z+\gamma$ data with the sum of the Standard Model prediction plus the estimated background. Although there is no significant deviation from SM expectations, we note the presence in our muon sample of an event with $E_T^{\gamma} \sim$ 64 GeV and $M_{Z+\gamma} \sim 188$ GeV/c^2.

We are in the process of extracting the cross section ratios $\mathcal{R}(W\gamma/W)$, $\mathcal{R}(Z\gamma/Z)$, $\mathcal{R}(W\gamma/Z\gamma)$ and $\mathcal{R}(W/Z)$ for the 1992-93 collider run. From the 1988-89 collider run, where an integrated luminosity of ~ 4 pb^{-1} was obtained, the $W+\gamma$ and $Z+\gamma$ cross sections and cross section ratios for $E_T^{\gamma} > 5$ GeV and $\Delta R_{\ell\gamma} > 0.7$ were extracted [19]. These cross section ratios and their SM predictions are summarized in Table 3.

CDF has published results for the e, μ and $e+\mu$ combined inclusive cross section ratio $\mathcal{R}(W/Z)$ from the 1988-89 collider run [20]. By taking ratios of these cross sections, as in the case of the $\mathcal{R}(W/Z)_\ell$ cross section ratio, many common experimental (and theoretical) uncertainties cancel [21]. The first and third cross section ratios, $\mathcal{R}(W\gamma/W)_\ell$ and $\mathcal{R}(W\gamma/Z\gamma)_\ell$, in the context of the SM are sensitive to the destructive interference between the u, t and $s-$channel Feynman amplitudes for the $W\gamma$ process [22]. The SM prediction for $\mathcal{R}(W\gamma/W)_\ell$, for our choice of photon cuts, is $\sim$ 1.0%, whereas if these events were due solely to radiative W decay, this ratio would instead be $\sim$ 0.6%. The second cross section ratio, $\mathcal{R}(Z\gamma/Z)_\ell$ is predicted to be $\sim$ 2.8% in the Standard Model. If these events were due solely to radiative Z decay, this ratio would be $\sim$ 2.1%. The third cross section ratio, that of $\mathcal{R}(W\gamma/Z\gamma)_\ell$ is predicted to be ~ 4.0 in the SM. If the photons observed in $W+\gamma$ events were due solely to final-state bremsstrahlung, this ratio is expected to be $\sim$ 2.5,

Cross Section Ratio	$\mathcal{R}_{expt}$	$\mathcal{R}_{SM}$
$\mathcal{R}(W\gamma/W)_e$	$0.9^{+0.7}_{-0.7}\%$	
$\mathcal{R}(W\gamma/W)_\mu$	$1.1^{+1.0}_{-1.0}\%$	$1.07 \pm 0.02\%$
$\mathcal{R}(W\gamma/W)_{e+\mu}$	$1.0^{+0.6}_{-0.6}\%$	
$\mathcal{R}(Z\gamma/Z)_e$	$3.3^{+2.8}_{-2.8}\%$	
$\mathcal{R}(Z\gamma/Z)_\mu$	$7.0^{+5.3}_{-5.3}\%$	$2.83 \pm 0.03\%$
$\mathcal{R}(Z\gamma/Z)_{e+\mu}$	$4.6^{+2.6}_{-2.6}\%$	
$\mathcal{R}(W\gamma/Z\gamma)_e$	$3.0^{+2.8}_{-3.0}$	
$\mathcal{R}(W\gamma/Z\gamma)_\mu$	$1.6^{+1.9}_{-1.6}$	4.05 ± 0.07
$\mathcal{R}(W\gamma/Z\gamma)_{e+\mu}$	$2.2^{+2.3}_{-1.5}$	
$\mathcal{R}(W/Z)_e$	$10.2^{+0.9}_{-0.9}$	
$\mathcal{R}(W/Z)_\mu$	$9.8^{+1.2}_{-1.2}$	10.69 ± 0.22
$\mathcal{R}(W/Z)_{e+\mu}$	$10.0^{+0.7}_{-0.7}$	

Table 3: W and Z cross section ratios for the 1988-89 data. The combined $(stat + syst)$ uncertainty associated with each quantity is given.

whereas if the photons observed in $Z + \gamma$ events were due solely to final-state bremsstrahlung, this ratio is expected to be ~ 5.4. The fourth cross section ratio is the inclusive W/Z cross section ratio, $\mathcal{R}(W/Z)_\ell$ which is predicted to be ~ 10.7. These cross section ratio results from the 1988-89 data are in good agreement with Standard Model expectations. We hope to present new cross section ratio results for the 1992-93 data in the near future.

We have obtained direct experimental limits on $WW\gamma$ ($ZZ\gamma$ and $Z\gamma\gamma$) anomalous couplings using the 1992-93 $W + \gamma$ ($Z + \gamma$) data samples, respectively. A binned maximum likelihood fit to the shape of the E_T^γ distribution for each of the combined $e + \mu$ data samples was carried out. Limits on anomalous couplings were found by comparing the photon E_T distribution to the sum of the estimated background plus the Monte Carlo signal prediction, calculating the likelihood that this sum would fluctuate to the observed number of events in each E_T bin. These probabilities are governed by Poisson statistics. The predicted number of events is convoluted with a Gaussian distribution to include the systematic uncertainty.

The 68%, 90% and 95% CL limit contours for the $\mathcal{CP}$-conserving $WW\gamma$ anomalous couplings $\Delta\kappa_\gamma$ and λ_γ are shown in Fig. 7a. A dipole form factor with a form factor scale $\Lambda_W = 1.5$ TeV is included in this analysis. Because of the nature of the $WW\gamma$ vertex function [1], the experimental results are insensitive to the form factor scale for $\Lambda_W > 0.3$ TeV. Tree-level S-matrix unitarity imposes constraints on the allowed values of $\Delta\kappa_\gamma$ and λ_γ in the $\bar{p}$-p $\rightarrow W\gamma$ and W^+W^- processes [23], as shown in Fig. 7a for $\Lambda_W = 1.5$ TeV. Unitarity is violated in the region outside these contours. Our 95% CL limit contour is well inside the unitarity constraints.

We obtain direct limits on $\mathcal{CP}$-conserving $WW\gamma$ anomalous couplings of $-2.3 < \Delta\kappa_\gamma < 2.2$ and $-0.7 < \lambda_\gamma < 0.7$ at 95% CL, assuming all other $WW\gamma$ anomalous couplings to be at their SM values. Similarly, we obtain direct limits on $\mathcal{CP}$-violating $WW\gamma$ anomalous couplings $\tilde{\kappa}_\gamma$ and $\tilde{\lambda}_\gamma$, which are within 3% of those obtained for $\Delta\kappa_\gamma$ and λ_γ, respectively. The 95% CL limit contour

is well inside the $\mathcal{CP}$-violating $W\gamma$ and WW unitarity constraints, the former (latter) of which is identical to (less restrictive than) the unitarity constraint for the $\mathcal{CP}$-conserving case.

The 68%, 90% and 95% CL limit contours for the $\mathcal{CP}$-conserving ($\mathcal{CP}$-violating) $ZZ\gamma$ and $Z\gamma\gamma$ anomalous couplings h_{30}^V and h_{40}^V (h_{10}^V and h_{20}^V) where $V = Z,\ \gamma$ are shown in Fig. 8. For the non-standard $Z^* \rightarrow Z + \gamma$ s-channel process, the effect of a generalized dipole form factor

$$h_i^V(\hat{s}, M_Z^2, 0) = \frac{h_{i0}^V}{(1 + \hat{s}/\Lambda_Z^2)^n} \tag{1}$$

where i = 1-4, $n = 3$ for $h_{1,3}^V$ ($n = 4$ for $h_{2,4}^V$) and the form factor scale is chosen to be Λ_Z, is included in this analysis. Because of the nature of the $ZZ\gamma$ and $Z\gamma\gamma$ vertex functions [1], the experimental results are strongly dependent on the form factor scale Λ_Z. Tree-level S-matrix unitarity imposes constraints on the allowed values of the h_{i0}^V parameters in the $\bar{\text{p}}$-p $\rightarrow Z + \gamma$ process [23], as shown in Fig. 8 for $\Lambda_Z = 500$ GeV. Unitarity is violated in the region outside these contours. Our 95% CL limit contours are well inside the unitarity constraints.

We obtain direct limits on $\mathcal{CP}$-conserving ($\mathcal{CP}$-violating) $ZZ\gamma$ anomalous couplings of $-3.0 < h_{30}^Z$ (h_{10}^Z) < 3.0 and $-0.7 < h_{40}^Z$ (h_{20}^Z) < 0.7 at 95% CL; and direct limits on $\mathcal{CP}$-conserving ($\mathcal{CP}$-violating) $Z\gamma\gamma$ anomalous couplings of $-3.1 < h_{30}^\gamma$ (h_{10}^γ) < 3.1 and $-0.8 < h_{40}^\gamma$ (h_{20}^γ) < 0.8 at 95% CL.

In the static limit (photon energy $k \rightarrow 0$), the $WW\gamma$ anomalous couplings, which are relativistic quantities, are related to the higher-order classical electromagnetic moments of the W boson [24] – the magnetic dipole moment μ_W, electric quadrupole moment Q_W^e, electric dipole moment d_W, magnetic quadrupole moment Q_W^m and the mean-squared charge radius, $<R_W^2>$ (with $\hbar = c = 1$) via:

$$\mu_W = \frac{e}{2M_W}(2 + \Delta\kappa_\gamma + \lambda_\gamma) = \frac{e}{2M_W} g_W \tag{2}$$

$$Q_W^e = -\frac{e}{M_W^2}(1 + \Delta\kappa_\gamma - \lambda_\gamma) = -\frac{e}{M_W^2} q_W^e \tag{3}$$

$$d_W = \frac{e}{2M_W}(\tilde{\kappa}_\gamma + \tilde{\lambda}_\gamma) = \frac{e}{2M_W}\delta_W \tag{4}$$

$$Q_W^m = -\frac{e}{M_W^2}(\tilde{\kappa}_\gamma - \tilde{\lambda}_\gamma) = -\frac{e}{M_W^2} q_W^m \tag{5}$$

$$<R_W^2> = \frac{1}{M_W^2}(1 + \Delta\kappa_\gamma + \lambda_\gamma) = \frac{1}{M_W^2} r_W^2 \tag{6}$$

The sign associated with each of these quantities indicates their orientation relative to the spin direction of the W^+ boson.

The limit contours for the $\mathcal{CP}$-conserving W boson EM moment quantities $g_W - 2$ and $q_W^e - 1$ are displayed in Fig. 7b. We obtain $-1.2 < g_W - 2 < 1.1$ for $q_W^e = 1$ and $-1.6 < q_W^e - 1 < 1.7$ for $g_W = 2$ and $-1.2 < r_W^2 - 1 < 1.2$ for $q_W^e = 1$ at 95% CL. We have also obtained direct limits on CP-violating electric dipole and magnetic quadrupole moments d_W and Q_W^m. The 95% CL limits on δ_W and q_W^m are within 3% of those obtained for $g_W - 2$ and $q_W^e - 1$, respectively. These results determine at almost 90% significance the sign of the magnetic dipole moment, μ_W, independent from the values of the other EM moments of the W boson.

The $ZZ\gamma$ anomalous couplings are related to the higher-order EM *transition* moments of the Z boson in the static limit (photon energy $k \to 0$) by [25]:

$$d_{Z_T} = -\frac{e}{M_Z}\frac{1}{\sqrt{2}}\frac{k^2}{M_Z^2}\left(h_{30}^Z - h_{40}^Z\right) = -\frac{e}{2M_Z}\delta_{Z_T} \quad (7)$$

$$Q_{Z_T}^m = \frac{e}{M_Z^2}\sqrt{10}\,(2h_{30}^Z) = \frac{e}{M_Z^2}q_{Z_T}^m \quad (8)$$

$$\mu_{Z_T} = -\frac{e}{M_Z}\frac{1}{\sqrt{2}}\frac{k^2}{M_Z^2}\left(h_{10}^Z - h_{20}^Z\right) = -\frac{e}{2M_Z}g_{Z_T} \quad (9)$$

$$Q_{Z_T}^e = \frac{e}{M_Z^2}\sqrt{10}\,(2h_{10}^Z) = \frac{e}{M_Z^2}q_{Z_T}^e \quad (10)$$

Setting direct experimental limits on δ_{Z_T} and g_{Z_T} is problematic because the $Z+\gamma$ photon energy spectrum is continuous, and sharply peaked at the experimental cutoff in E_T^γ. The factor (k^2/M_Z^2) in the definition of these transition moments is rather ill-defined, experimentally. Hence, we define the following variables for these two quantities:

$$\delta_{Z_T}^* \equiv \delta_{Z_T}\left[\frac{M_Z^2}{k^2}\right] = \sqrt{2}\left(h_{30}^Z - h_{40}^Z\right) \quad (11)$$

$$g_{Z_T}^* \equiv g_{Z_T}\left[\frac{M_Z^2}{k^2}\right] = \sqrt{2}\left(h_{10}^Z - h_{20}^Z\right) \quad (12)$$

The limit contours for the $\mathcal{CP}$-conserving ($\mathcal{CP}$-violating) Z boson EM transition moment quantities $\delta_{Z_T}^*$ and $q_{Z_T}^m$ ($g_{Z_T}^*$ and $q_{Z_T}^e$) are displayed in Fig. 9 for a form factor scale $\Lambda_Z = 500$ GeV. The $ZZ\gamma$ unitarity constraint for this form factor scale is also shown in the figure. We obtain direct limits on the $\mathcal{CP}$-conserving ($\mathcal{CP}$-violating) $ZZ\gamma$ transition moments of $-1.1 < \delta_{Z_T}^*\ (g_{Z_T}^*) < 1.0$ and $-6.0 < q_{Z_T}^m\ (q_{Z_T}^e) < 6.0$ at 95% CL. No such analogous relations exist for $Z\gamma\gamma$ anomalous couplings, since in the $\gamma^* \to Z+\gamma$ process, the virtual photon is (very) far off the mass shell.

The direct experimental limits on $WW\gamma$, $ZZ\gamma$ and $Z\gamma\gamma$ anomalous couplings and W (Z) static (transition) EM moments obtained from the 1992-93 data represent a factor of $\sim$ 3-fold improvement over those extracted from the 1988-89 data [19].

W^+W^-, WZ and ZZ Boson Pair Production at CDF

WW, WZ and ZZ boson pair candidates were also obtained from the inclusive electron and muon W and Z data samples using the same W/Z event selection criteria. To increase the sensitivity, this analysis also included electron W candidates where the W decay electron was located in the PEM calorimeter. This inclusive W data sample was obtained with a PEM electron trigger which required $E_T > 20$ GeV. Offline, isolated PEM electron W candidates were required to be in a good fiducial region of the PEM calorimeter, have $E_T > 20$ GeV, and be isolated. To further increase the sensitivity of the measurement, events in which the second boson decayed either leptonically or hadronically where used.

In the presence of anomalous couplings, the amplitudes for $WW\gamma$, WWZ and/or ZZZ are strongly $\hat{s}$-dependent, leading to an excess rate of production for high-P_T di-boson pairs. This kinematic feature can be used to dramatically suppress the W/Z+QCD jet(s) background to the WW, WZ and ZZ processes, where one boson decays leptonically, the other hadronically. The

W/Z+QCD jet background is primarily in the low jet-E_T region. For di-boson decay modes involving hadronic decays of W/Z bosons, two jets with $E_T^j > 30$ GeV and $|\eta_j| < 2.5$ were required. Jet energy response corrections were applied to each jet before applying this cut.

For WW, $WZ \to \ell\nu\ jj$ candidates, we required $M_T^{\ell\nu} > 40$ GeV/c^2, the jet-jet invariant mass to be within $60 < M_{jj} < 110$ GeV/c^2 and $P_T^{jj} > 130$ GeV/c. The P_T^{jj} cut strongly suppresses W/Z+QCD jet background, but also suppresses much of the SM di-boson signal in these decay channels. For ZW, $ZZ \to \ell^+\ell^-\ jj$ candidates, the di-lepton pair mass was required to be within $70 < M_{\ell^+\ell^-} < 110$ GeV/c^2, the jet-jet invariant mass to be within $60 < M_{jj} < 110$ GeV/c^2 and $P_T^{jj} > 100$ GeV/c.

Using these event selection criteria, no ZZ, $ZW \to \ell^+\ell^-\ jj$ and one electron WW, $WZ \to \ell\nu\ jj$ candidate were found. Figures 10-11 show the CTC ($r-\phi$) and calorimeter (lego) views of the $\bar{\rm p}{\rm p} \to ZW \to e^+e^-\ e^+\nu_e$ boson pair candidate.

The SM prediction for each of these processes was obtained using the Zeppenfeld weak boson pair Monte Carlo event generator [26] and QFL CDF detector simulation, using MT B2 structure functions [14]. The (fractional) uncertainty associated with each of these SM predictions is $\sim$ 14-15% due to uncertainties associated with the P_T distribution for the boson pair, higher-order QCD corrections to these processes [27], structure function choice, jet E_T scale and jet resolution uncertainties, as well as the uncertainty in the luminosity determination, lepton trigger and identification efficiencies and the finite statistics associated with Monte Carlo simulation.

Direct limits on $\mathcal{CP}$-conserving and $\mathcal{CP}$-violating $WW\gamma$ and WWZ anomalous couplings for each of the WW and WZ channels were obtained using the di-boson Monte Carlo to obtain the predicted event yield in each channel, and then computing the probability that the experiment would find the observed number of events or fewer in that channel, (conservatively) assuming the observed number of events in each channel to be pure signal. The probability distribution used was the convolution of a Poisson distribution smeared by a Gaussian to include the systematic uncertainty associated with the predicted event yield.

The greatest sensitivity occurs in the WW, $WZ \to \ell\nu\ jj$ channel, as shown in Fig. 12 for $\mathcal{CP}$-conserving $WW\gamma/WWZ$ anomalous couplings, assuming $\Delta\kappa_\gamma = \Delta\kappa_Z = \Delta\kappa$ and $\lambda_\gamma = \lambda_Z = \lambda$. If only one non-zero $WW\gamma/WWZ$ anomalous coupling is considered at a time, the limits are $-1.0 < \Delta\kappa < 1.1$ and $-0.8 < \lambda < 0.8$ at 95% CL for a dipole form factor and $\Lambda_W = 1.5$ TeV. The $WW\gamma/WWZ$ unitarity constraint [23] is also shown in this figure. The region exterior to the unitarity contour is excluded. The $\Delta\kappa$-λ 95% CL limit contour is just inside the unitarity constraint for $\Lambda_W = 1.5$ TeV. If $\Delta\kappa_\gamma \neq \Delta\kappa_Z$, we obtain $-2.5 < \Delta\kappa_\gamma < 2.8$ for $\Delta\kappa_Z = 0$ and $-1.3 < \Delta\kappa_Z < 1.4$ for $\Delta\kappa_\gamma = 0$ at 95% CL for $\Lambda_W = 1.5$ TeV. For the $ZW \to \ell^+\ell^-\ jj$ channel, we obtain $-8.6 < \Delta\kappa_Z < 9.0$ for $\lambda_Z = 0$ and $-1.7 < \lambda_Z < 1.7$ for $\Delta\kappa_Z = 0$.

We obtain direct limits on $\mathcal{CP}$-violating $WW\gamma/WWZ$ anomalous couplings, as shown in Fig. 13 for the WW, $WZ \to \ell\nu\ jj$ channel, assuming $\tilde{\kappa}_\gamma = \tilde{\kappa}_Z = \tilde{\kappa}$ and $\tilde{\lambda}_\gamma = \tilde{\lambda}_Z = \tilde{\lambda}$. We find $-3.4 < \tilde{\kappa} < 3.3$ for $\tilde{\lambda} = 0$ and $-0.8 < \tilde{\lambda} < 0.8$ for $\tilde{\kappa} = 0$ at 95% CL, for a form factor scale of $\Lambda_W = 1.5$ TeV.

Work on extracting direct experimental limits for $WW\gamma$ and WWZ anomalous couplings using all-leptonic final states is in progress; as is work on extracting direct limits on $ZZ\gamma$ and ZZZ anomalous couplings from the $ZZ \to \ell^+\ell^-\ jj$ and $ZZ \to \ell^+\ell^-\ \ell^+\ell^-$ di-boson channels. For two

on-shell Z's in the final state, Bose symmetry allows only two couplings – one $\mathcal{CP}$-conserving, the other $\mathcal{CP}$-violating [1]. If at least one of the final state Z bosons is off shell, five additional couplings are possible, as in the case for $WW\gamma/WWZ$ vertices.

Summary and Future Prospects

From ~ 20 pb^{-1} data, we have observed 25 $e+\mu$ $W+\gamma$ candidate events and 8 $e+\mu$ $Z+\gamma$ candidate events, with backgrounds of 8.5 ± 1.9 $(stat + syst)$ and 0.5 ± 0.2 $(stat + syst)$ events, respectively. Using these data samples, we have extracted measurements of the production cross section $\times$ decay branching ratios of $\sigma \cdot B(W+\gamma)_{e+\mu} = 13.2 \pm 4.4$ $(stat + syst)$ and $\sigma \cdot B(Z+\gamma)_{e+\mu} = 5.1 \pm 1.9$ $(stat + syst)$. Work is in progress to repeat the 1988-89 data analysis to obtain improved results on the cross section ratios $\mathcal{R}(W\gamma/W)$, $\mathcal{R}(Z\gamma/Z)$, $\mathcal{R}(W\gamma/Z\gamma)$ and $\mathcal{R}(W/Z)$ with the 1992-93 data.

From the combined $e+\mu$ data samples, we have obtained direct experimental limits on $WW\gamma$, $ZZ\gamma$ and $Z\gamma\gamma$ anomalous couplings. We obtain direct limits on $\mathcal{CP}$-conserving $WW\gamma$ anomalous couplings of $-2.3 < \Delta\kappa_\gamma < 2.2$ and $-0.7 < \lambda_\gamma < 0.7$ at 95% CL, assuming all other $WW\gamma$ anomalous couplings to be at their SM values. These results are sensitive to a form factor scale up to $\Lambda_W = 1.5$ TeV. Similarly, we obtain direct limits on $\mathcal{CP}$-violating $WW\gamma$ anomalous couplings $\tilde{\kappa}_\gamma$ and $\tilde{\lambda}_\gamma$, which are within 3% of those obtained for $\Delta\kappa_\gamma$ and λ_γ, respectively. We obtain direct limits on $\mathcal{CP}$-conserving ($\mathcal{CP}$-violating) $ZZ\gamma$ and $Z\gamma\gamma$ anomalous couplings of $-3.0 < h^Z_{30}$ $(h^Z_{10}) < 3.0$ and $-0.7 < h^Z_{40}$ $(h^Z_{20}) < 0.7$; and $-3.1 < h^\gamma_{30}$ $(h^\gamma_{10}) < 3.1$ and $-0.8 < h^\gamma_{40}$ $(h^\gamma_{20}) < 0.8$ at 95% CL. These results are sensitive to a form factor scale up to $\Lambda_Z = 500$ GeV.

In the static limit, the direct experimental limits on $WW\gamma$ ($ZZ\gamma$) anomalous couplings are related to bounds on the higher-order static (transition) EM moments of the W (Z) bosons, respectively. For the W boson, we obtain limits on the magnetic dipole moment and electric quadrupole moments of $-1.2 < g_W - 2 < 1.1$ for $q^e_W = 1$ and $-1.6 < q^e_W - 1 < 1.7$ for $g_W = 2$ and $-1.2 < r^2_W - 1 < 1.2$ for $q^e_W = 1$ at 95% CL. We have also obtained direct limits on CP-violating electric dipole and magnetic quadrupole moments d_W and Q^m_W. The 95% CL limits on δ_W and q^m_W are within 3% of those obtained for $g_W - 2$ and $q^e_W - 1$, respectively. These results determine at almost 90% significance the sign of the magnetic dipole moment, μ_W, independent from the values of the other EM moments of the W boson. For the Z boson, we obtain direct limits on the $\mathcal{CP}$-conserving ($\mathcal{CP}$-violating) $ZZ\gamma$ transition moments of $-1.1 < \delta^*_{Z_T}$ $(g^*_{Z_T}) < 1.0$ and $-6.0 < q^m_{Z_T}$ $(q^e_{Z_T}) < 6.0$ at 95% CL.

These results are in good agreement with SM expectations. Work is in progress to extend the photon coverage into the plug EM calorimeter region to increase the statistics of the run Ia $W+\gamma$ and $Z+\gamma$ data samples, which will be particularly important for studying the photon-lepton pseudorapidity correlation and the predicted dip in the $\Delta\eta_{\gamma-\ell^\pm}$ distribution at $\sim \mp 0.3$ due to the SM radiation amplitude zero in $\bar{p}$-p $\rightarrow W+\gamma$ production.

From the "heavy" weak boson pair analysis, the greatest sensitivity to $WW\gamma$ and WWZ anomalous couplings occurs in the WW, $WZ \rightarrow \ell\nu\, jj$ channel, We obtain direct experimental limits on $\mathcal{CP}$-conserving $WW\gamma/WWZ$ anomalous couplings, assuming $\Delta\kappa_\gamma = \Delta\kappa_Z = \Delta\kappa$ and $\lambda_\gamma = \lambda_Z = \lambda$. If only one non-zero $WW\gamma/WWZ$ anomalous coupling is considered at a time, the limits are $-1.0 < \Delta\kappa < +1.1$ and $-0.8 < \lambda < 0.8$ at 95% CL for $\Lambda_W = 1.5$ TeV. If $\Delta\kappa_\gamma \neq \Delta\kappa_Z$, we obtain $-2.5 < \Delta\kappa_\gamma < 2.8$ for $\Delta\kappa_Z = 0$ and $-1.3 < \Delta\kappa_Z < 1.4$ for $\Delta\kappa_\gamma = 0$ at 95% CL for $\Lambda_W = 1.5$ TeV.

For the $ZW \rightarrow \ell^+\ell^- jj$ channel, we obtain $-8.6 < \Delta\kappa_Z < 9.0$ for $\lambda_Z = 0$ and $-1.7 < \lambda_Z < 1.7$ for $\Delta\kappa_Z = 0$.

We have also obtained direct limits on $\mathcal{CP}$-violating $WW\gamma/WWZ$ anomalous couplings, using the $WW, WZ \rightarrow \ell\nu\, jj$ channel, assuming $\tilde{\kappa}_\gamma = \tilde{\kappa}_Z = \tilde{\kappa}$ and $\tilde{\lambda}_\gamma = \tilde{\lambda}_Z = \tilde{\lambda}$. We find $-3.4 < \tilde{\kappa} < 3.3$ for $\tilde{\lambda} = 0$ and $-0.8 < \tilde{\lambda} < 0.8$ for $\tilde{\kappa} = 0$ at 95% CL, for a form factor scale of $\Lambda_W = 1.5$ TeV. These results are also in good agreement with SM expectations.

Work on extracting direct experimental limits on $ZZ\gamma$ and ZZZ anomalous couplings from $ZZ \rightarrow \ell^+\ell^-\ \ell^+\ell^-$ and $ZZ \rightarrow \ell^+\ell^-\ jj$ di-boson channels is in progress. When the analysis of the run Ia di-boson data is completed, we plan to combine limits on anomalous couplings obtained from $W + \gamma$ and $Z + \gamma$ data with those obtained from the "heavy" boson pair data. Work is also in progress to relax the stringent cuts used in the latter analysis to improve our acceptance for the SM signal in each of the various di-boson decay channels.

Tevatron collider run Ib is currently in progress. We hope to accumulate ~ 75 pb^{-1} data by the end of the run (June, 1995), increasing the statistics in each of these data samples by a factor of nearly four. Beyond this, we anticipate significantly larger di-boson data samples with Tevatron collider Run II, and the commissioning of the Main Injector at the end of this decade, where data samples of ~ 1 fb^{-1} integrated luminosity are hoped for.

We thank the Fermilab staff and the technical staffs of the participating institutions for their vital contributions. This work was supported by the U.S. Department of Energy and National Science Foundation; the Italian Istituto Nazionale di Fisica Nucleare; the Ministry of Education, Science and Culture of Japan; the Natural Sciences and Engineering Research Council of Canada; the National Science Council of the Republic of China; the A. P. Sloan Foundation; and the Alexander von Humboldt-Stiftung. We thank U. Baur, F. Boudjema and D. Zeppenfeld for many helpful discussions.

References

[1] K. Hagiwara, R. D. Peccei, D. Zeppenfeld, and K. Hikasa, Nucl. Phys. B **282**, 253 (1987); K. Gaemers and G. Gounaris, Z. Phys. C **1**, 259 (1979); K. Hagiwara, J. Woodside and D. Zeppenfeld, Phys. Rev. D **41**, 2113 (1990).

[2] K.O. Mikaelian, Phys. Rev. D **17**, 750 (1978); K.O. Mikaelian, M.A. Samuel and D. Sahdev, Phys. Rev. Lett. **43**, 746 (1979); R.W. Brown, K.O. Mikaelian and D. Sahdev, Phys. Rev. D **20**, 1164 (1979); T.R. Grose and K.O. Mikaelian, Phys. Rev. D **23**, 123 (1981); C.J. Goebel, F. Halzen and J.P. Leveille, Phys. Rev. D **23**, 2682 (1981); S.J. Brodsky and R.W. Brown, Phys. Rev. Lett. **49**, 966 (1982); M.A. Samuel, Phys. Rev. D **27**, 2724 (1983); R.W. Brown, K.L. Kowalski and S.J. Brodsky, Phys. Rev. D **28**, 624 (1983); R.W. Brown and K.L. Kowalski, Phys. Rev. D **29**, 2100 (1984).

[3] U. Baur, S. Errede and G. Landsberg, to appear in Phys. Rev. D; U. Baur, S. Errede and G. Landsberg, in *The Proceedings of the Workshop on Physics at Current Accelerators and Supercolliders*, p. 211-217, edited by J. Hewett, A. White and D. Zeppenfeld (Argonne, June 2-5, 1993).

[4] U. Baur, T. Han and J. Ohnemus, FSU-HEP-940307, UCD-94-5, hep-ph/9403248 (March, 1994) (Submitted to Phys. Rev. D, 1994).

[5] F.M. Renard, Nucl. Phys. B **196**, 93 (1982); R. Barbieri, H. Harari and M. Leurer, Phys. Lett. B **141**, 455 (1985); J.P. Eboli, A.V. Olinto, Phys. Rev. D **38**, 3461 (1988).

[6] A. DeRujula, *et al.*, Nucl. Phys. B **384**, 3 (1992); A. Falk, M. Luke and E. Simmons, Nucl. Phys. B **365**, 523 (1991); J. Bagger, S. Dawson and G. Valencia, Nucl. Phys. B **399**, 364 (1993); K. Hagiwara, *et al.*, Phys. Rev. D **2182** (1993); C. Burgess and D. London, Phys. Rev. D **48**, 4337 (1993); C. Artz, M.B. Einhorn and J. Wudka, Phys. Rev. D **49**, 1370 (1994).

[7] J. M. Cornwall, D. N. Levin and G. Tiktopoulos, Phys. Rev. Lett. **30**, 1268 (1973); Phys. Rev. D **10**, 1145 (1974); C. H. Llewellyn Smith, Phys. Lett. B **46**, 233 (1973); S. D. Joglekar, Ann. of Phys. **83**, 427 (1974).

[8] F. Abe *et al.*, (the CDF Collaboration), Nucl. Instr. Methods A **271**, 387 (1988).

[9] See *e.g.* F. Abe *et al.*, (the CDF Collaboration), Phys. Rev. D **44**, 29 (1991); and Phys. Rev. Lett. **68**, 3398 (1992).

[10] See *e.g.* F. Abe *et al.*, (the CDF Collaboration), Phys. Rev. D **44**, 29 (1991); and Phys. Rev. Lett. **69**, 28 (1992).

[11] F. A. Berends, W.T. Giele, H. Kuijf and B. Tausk, Nucl. Phys. B **357**, 32 (1991).

[12] U. Baur and E.L. Berger, Phys. Rev. D **47**, 4889 (1993).

[13] U. Baur and E.L. Berger, Phys. Rev. D **41**, 1476 (1990); See also U. Baur and D. Zeppenfeld, Nucl. Phys. B **308**, 127 (1988).

[14] A.D. Martin, R.G. Roberts and W.J. Stirling, Phys. Rev. D **47**, 867 (1993); and J.G. Morfin and Wu-Ki Tung, Z. Phys. C **52**, 13 (1991), incorporated into CERN PDFLIB version 4.15, H. Plothow-Besch, Computer Phys. Commun. **75**, 396 (1993).

[15] F. Abe, *et al.*, (the CDF Collaboration), Submitted to Phys. Rev. Lett. (1994).

[16] F. Abe, *et al.*, (the CDF Collaboration), Phys. Rev. Lett. **67**, 2937 (1991).

[17] J. Ohnemus, Phys. Rev. D **47**, 940 (1993); U. Baur, T. Han and J. Ohnemus, Phys. Rev. D **48**, 5140 (1993); See also J. Smith, D. Thomas and W.L. van Neerven, Z. Phys. C **44**, 267 (1989); S. Mendoza, J. Smith and W.L. van Neerven, Phys. Rev. D **47**, 3913 (1993);

[18] The cluster transverse mass (minimum invariant mass) of the $W+\gamma$ system is defined as

$$M_{CT}^{W\gamma} \equiv \left\{ \left[\left(M_{\ell\gamma}^2 + |\vec{\mathbf{P}}_T^{\gamma} + \vec{\mathbf{P}}_T^{\ell}|^2 \right)^{\frac{1}{2}} + |\vec{\mathbf{P}}_T^{\bar{\nu}_\ell}| \right]^2 - |\vec{\mathbf{P}}_T^{\gamma} + \vec{\mathbf{P}}_T^{\ell} + \vec{\mathbf{P}}_T^{\bar{\nu}_\ell}|^2 \right\}^{\frac{1}{2}}$$

where $M_{\ell\gamma}$ is the invariant mass of the lepton-photon system.

[19] F. Abe *et al.*, (the CDF Collaboration), to be submitted to Phys. Rev. D (1994).

[20] F. Abe *et al.*, (the CDF Collaboration), Phys. Rev. Lett. **62**, 1005 (1989); F. Abe *et al.*, (the CDF Collaboration), Phys. Rev. D **44**, 29 (1991); F. Abe *et al.*, (the CDF Collaboration), Phys. Rev. Lett. **69**, 28 (1992); See also F. Abe *et al.*, (the CDF Collaboration), Phys. Rev. Lett. **64**, 152 (1990); F. Abe *et al.*, (the CDF Collaboration), Phys. Rev. Lett. **68**, 3398 (1992).

[21] F. Halzen, and K. Mursula, Phys. Rev. Lett. **51**, 857 (1983); K. Hikasa, Phys. Rev. D **29**, 1939 (1984); N.G. Deshpande, *et al.*, Phys. Rev. Lett. **54**, 1757 (1985); A.D. Martin, R.G. Roberts and W.J. Stirling, Phys. Lett. B **189**, 220 (1987); E.L. Berger, F. Halzen, C.S. Kim and S. Willenbrock, Phys. Rev. D **40**, 83 (1989).

[22] U. Baur, S. Errede and J. Ohnemus, Phys. Rev. D **48**, 4103 (1993).

[23] U. Baur and D. Zeppenfeld, Phys. Lett. B **201**, 383 (1988).

[24] H. Aronson, Phys. Rev. **186**, 1434 (1969); K.J. Kim and Y.-S. Tsai, Phys. Rev. D**7**, 3710 (1973). See also: T.D. Lee and C.N. Yang, Phys. Rev. **128**, 885 (1962); L.D. Landau and E.M. Lifshitz, *Quantum Mechanics* (Addison-Wesley Publishing Co, Inc., Reading, MA, 1965), p. 262; and D.R. Yennie, M.M. Lévy and D.G. Ravenhall, Rev. Mod. Phys. **29**, 144 (1957); L. Durand III, P.C. DeCelles and R.B. Marr, Phys. Rev. **126**, 1882 (1962).

[25] F. Boudjema, private communication.

[26] Weak boson pair production event generator program provided by D. Zeppenfeld, private communication.

[27] J. Ohnemus, UCD-94-9 (1994) (Submitted to Phys. Rev. D, 1994); J. Ohnemus, Phys. Rev. D **41**, 2113 (1990); J. Ohnemus and J.F. Owens, Phys. Rev. D **43**, 3626 (1991) and J. Ohnemus, Phys. Rev. D **44**, 3477 (1991).

[28] F. Abe, *et al.*, (the CDF Collaboration), Fermilab PUB-94/097E, April, 1994, (Submitted to Phys. Rev. D, 1994).

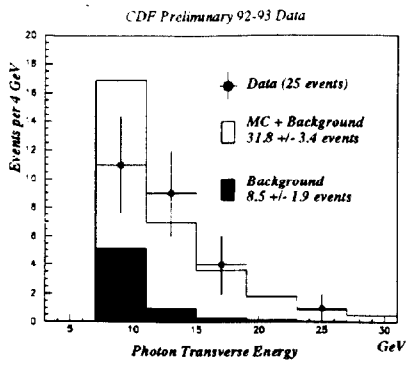

Figure 1: E_T distribution of central photon candidates in $W\gamma$ events. The prediction for the SM signal has been added to the background prediction.

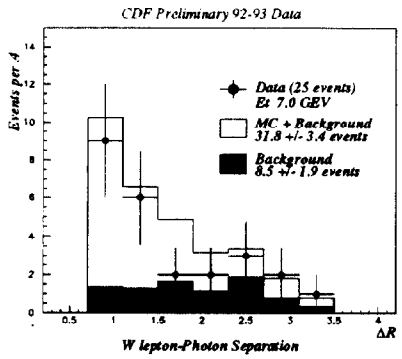

Figure 2: Angular separation $\Delta R_{\ell\gamma}$ of the photon candidate and the charged lepton from the W decay. The prediction for the SM signal has been added to the background prediction.

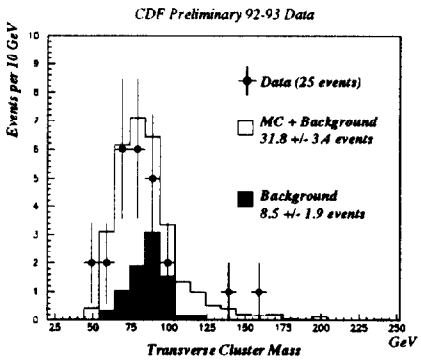

Figure 3: Cluster transverse mass M_{CT}^{W} of the W decay leptons and the photon. The prediction for the SM signal has been added to the background prediction.

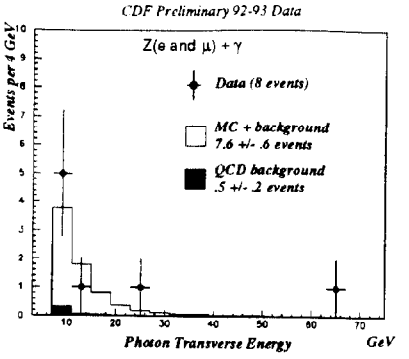

Figure 4: E_T distribution of central photon candidates in $W\gamma$ events. The prediction for the SM signal has been added to the background prediction.

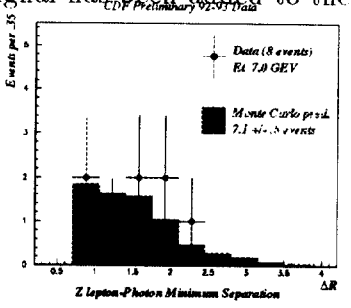

Figure 5: Angular separation $\Delta R_{\ell\gamma}^{\min}$ of the photon candidate and the nearest charged lepton from the Z decay. The prediction for the SM signal has been added to the background prediction.

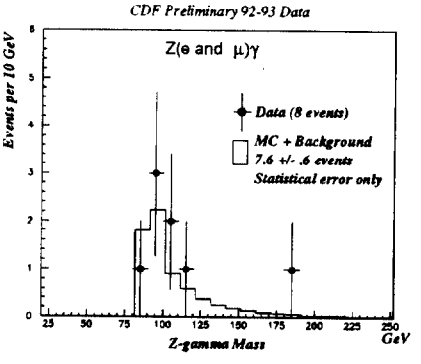

Figure 6: Three-body mass $M_{\ell^+\ell^-\gamma}$ of the Z decay leptons and the photon. The prediction for the SM signal has been added to the background prediction.

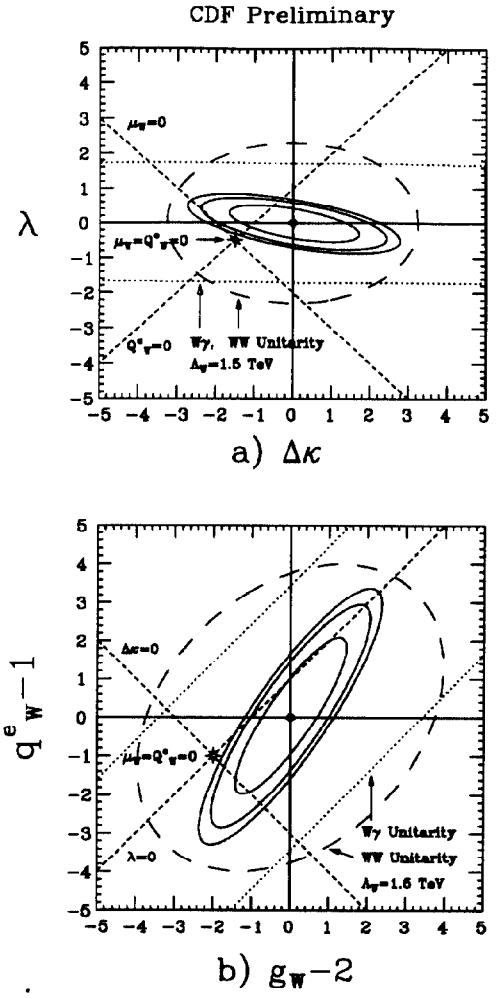

Figure 7: Direct limits on $\mathcal{CP}$-conserving $WW\gamma$ anomalous couplings (a) and on the static $\mathcal{CP}$-conserving EM multipole moments of the W boson (b) for the combined $e + \mu$ $W + \gamma$ data sample. In each figure, the star indicates the point where these EM moments vanish. The solid ellipses show the 68%, 90% and 95% CL limit contours. The W^+W^- and $W\gamma$ unitarity limits for a form factor scale Λ_W = 1.5 TeV are indicated by dashed and dotted curves, respectively.

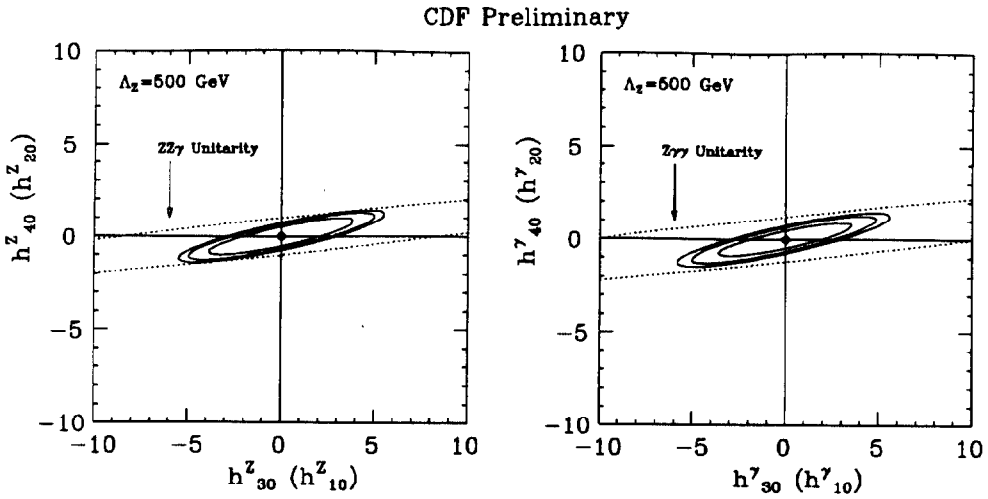

Figure 8: Direct limits on $\mathcal{CP}$-conserving ($\mathcal{CP}$-violating) $ZZ\gamma$ and $Z\gamma\gamma$ couplings for the combined $e+\mu$ $Z+\gamma$ data sample. The solid ellipses show the 68%, 90% and 95% CL limit contours. The $ZZ\gamma$ and $Z\gamma\gamma$ unitarity limits for a form factor scale $\Lambda_Z = 500$ GeV are indicated by the dotted contours.

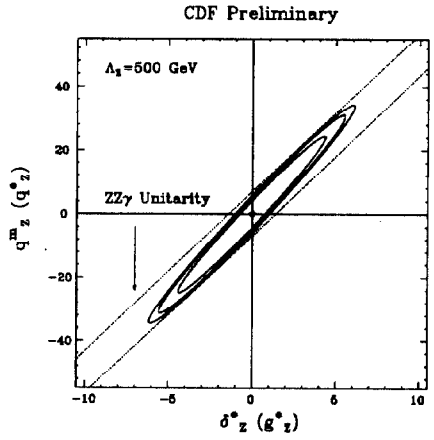

Figure 9: Direct limits on $\mathcal{CP}$-conserving ($\mathcal{CP}$-violating) $ZZ\gamma$ transition multipole moments for the combined $e+\mu$ $Z+\gamma$ data sample. The solid ellipses show the 68%, 90% and 95% CL limit contours. The $ZZ\gamma$ unitarity limits for a form factor scale $\Lambda_Z = 500$ GeV are indicated by the dotted contour.

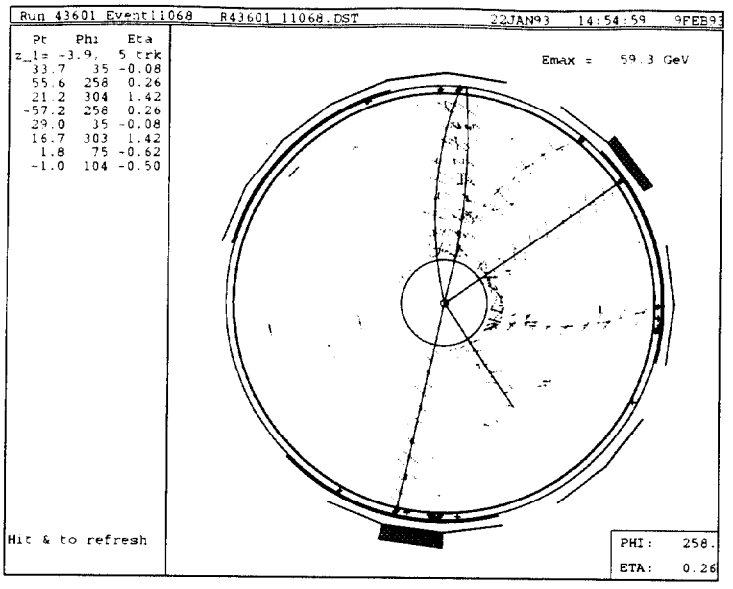

Figure 10: CTC $(r-\phi)$ view of $ZW \rightarrow e^+e^-\ e^+\nu_e$ candidate. The central e^+e^- pair has an invariant mass consistent with $Z \rightarrow e^+e^-$, the e^+ in the plug EM calorimeter and $\not\!\!E_T$ have transverse mass consistent with $W^+ \rightarrow e^+\nu_e$.

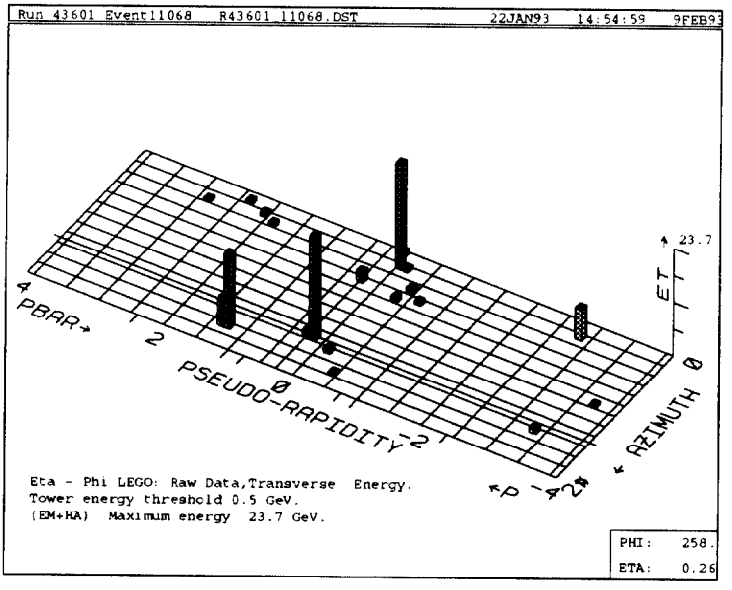

Figure 11: Calorimeter (lego) view of $WZ \rightarrow e^+e^-\ e^+\nu_e$ candidate.

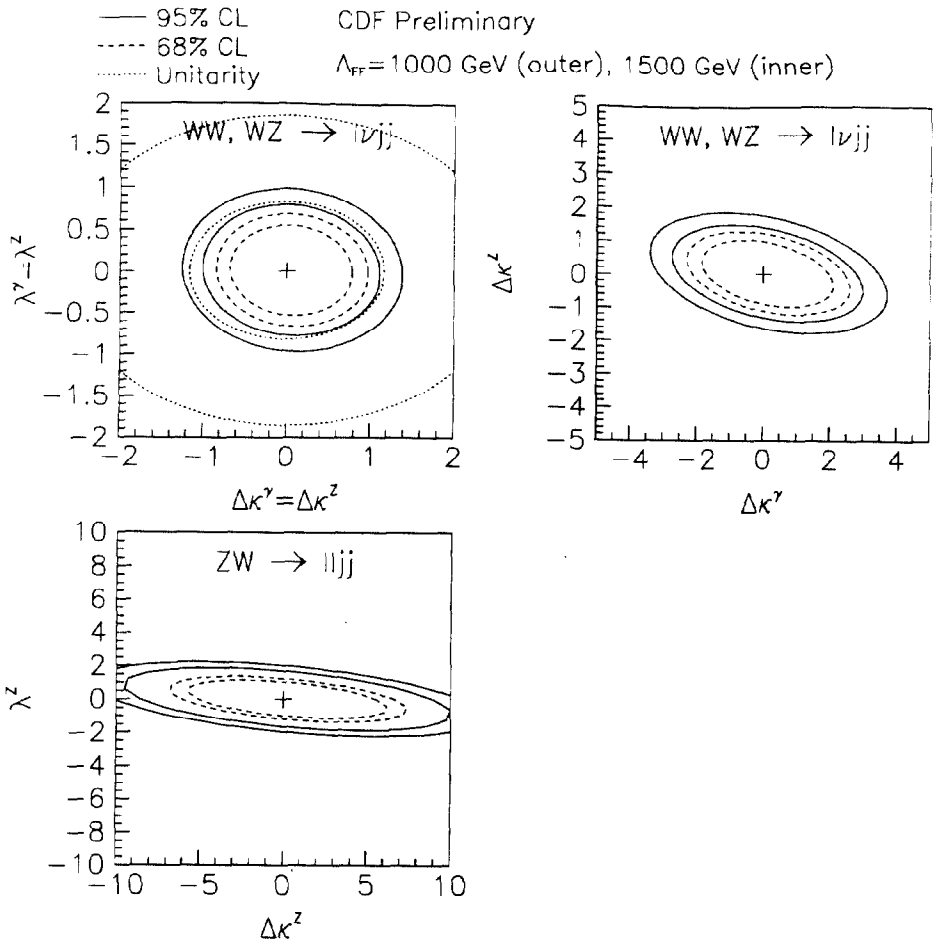

Figure 12: Limits on $\mathcal{CP}$-conserving $WW\gamma$ and WWZ anomalous couplings from WW or WZ production, where one boson decays leptonically and the other hadronically. The dashed (solid) ellipses show the 68% (95% CL) limit contours. The unitarity limits for a form factor scale $\Lambda_W = 1.5$ TeV are indicated by the dotted contour.

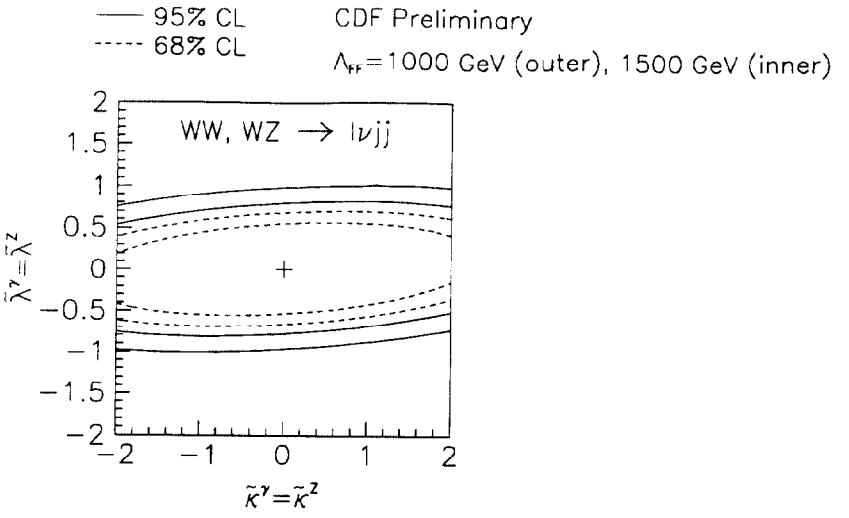

Figure 13: Limits on $\mathcal{CP}$-violating $WW\gamma$ and WWZ anomalous couplings from WW or WZ production, where one W decays leptonically and the accompanying W or Z decays hadronically. The dashed (solid) ellipses show the 68% (95% CL) limit contours.